A Comparative Molecular Field Analysis of Propafenone-type Modulators of Cancer Multidrug Resistance§

Ilza K. Pajeva[1] and Michael Wiese*[2]

[1]Center of Biomedical Engineering, Bulgarian Academy of Sciences, Acad. G. Bonchev Str., Bl. 105, BG-1113 Sofia, Bulgaria
[2]Department of Pharmacy, Martin-Luther-University, Wolfgang-Langenbeck-Str. 4, D-06120 Halle/Saale, Germany

Abstract

The presented 3D-QSAR is based on literature data of daunomycin MTT cytotoxicity and rhodamine-123 efflux inhibition activity in CCRF-CEMvcr1000 multidrug resistant (MDR) tumor cell line of 28 compounds from the propafenone and benzofuran classes. A systematic conformational search of the most active compounds in their classes was performed and the resulting minimum energy conformations were used in the further analysis. The structures were superimposed according to two different alignment rules using both, rms and field fit alignment techniques. A number of ComFA models were derived using the standard CoMFA steric and electrostatic fields as well as hydrophobic fields. Most of the models were statistically significant and highly predictive. Better CoMFA models were obtained for MTT cytotoxicity assay than for rhodamine-123 efflux inhibition assay activity data. The hydrophobic fields alone and in combination with the steric and both, (steric and electrostatic) fields yielded the models with the highest cross-validated coefficients of explained variance. The results show that the differences in MDR-modulating activity of the compounds of different classes can be explained if based on hydrophobicity as a space directed molecular property.

1 Introduction

Nowadays multidrug resistance (MDR) is considered to be the major reason for failure in the chemotherapy of cancer. Many structurally unrelated substances, called MDR modulators or reverters, have been found to enhance the cytotoxic activity of the antitumor drugs in MDR cells [1]. In general, they are supposed to inhibit the efflux activity of the membrane transport protein P-glycoprotein (P-gp) that pumps the cytotoxic agent out of the tumor cell decreasing in this way its intracellular accumulation and cytotoxicity respectively. The most widespread hypothesis about the mechanism of the P-gp associated MDR reversal presumes a competition between the cytotoxic agent and MDR modulator for the same binding site or sites on P-gp [2]. It is well recognized that the MDR modulators share common physicochemical characteristics – they are lipophilic and mostly positively charged at physiological pH [3]. The majority of them are cationic amphiphilic compounds that usually possess an aromatic ring system and a basic tertiary nitrogen at a given distance from the aromatic system. A number of studies report qualitative structure-activity relationships of different MDR modulators in order to identify some more specific structural features in addition to their commonly shared physicochemical characteristics [4–6].

Recently we performed a QSAR analysis of phenothiazine-type MDR modulators and quantitatively estimated several structural features of significant importance for their anti-MDR activity *in vitro* in MCF-7/DOX tumor cells [7]. The subsequent conformational and molecular modeling study of the MDR reverters trans- and cis-flupentixol, based on NMR data of the stereoisomers in a membrane lipid

* To receive all correspondence
§Supported by Deutsche Forschungsgemeinshaft, grant no. 436 BUL-112/8/97 and National Science Fund, Bulgarian Ministry of Education, Science and Technology

Key words: CoMFA, resistance modulator, multidrug resistance, Propafenone

Abbreviations and symbols: MDR, multidrug resistance; P-gp, P-glycoprotein; DOX, doxorubicin; VCR, vincristine; MTT, 3-(4,5-dimethylthiazol-2-yl)-2,5-diphenyltetrazolium bromide; Rh, rhodamine-123; NMR, nuclear magnetic resonance; PCA, principal component analysis; CoMFA, comparative molecular field analysis; σ_{min}, threshold column filtering in CoMFA; PLS, partial least squares; Q^2_{cv}, squared correlation coefficient of predictions by "leave one out" procedure; N_{opt}, optimal number of components extracted by PLS; SEP_{cv}, standard error of prediction; R^2, coefficient of multiple determination; s, standard deviation of estimation; F, the F-value.

  0931-8771/98/0408-0301 $17.50+.50/0

environment, pointed to the space directed differences in the molecular fields of the drugs being responsible for the differences in their anti-MDR activity [8]. These results motivated our further 3D-QSAR study on 40 phenothiazines, thioxanthenes and structurally related MDR modulators by the CoMFA approach [9]. A number of highly predictive models were obtained and interpreted in terms of the steric, electrostatic and hydrophobic molecular fields of the drugs. The results pointed to the key role of hydrophobicity as a space directed property for explaining the differences in their MDR modulating activity. To further proof this suggestion we directed our attention to other classes of MDR modulators. Data from Ecker and coworkers were selected from the literature as offering various and highly convincing biological results on MDR reversing activity *in vitro* for a number of newly synthesized propafenone-type MDR modulators [10,11].

In this paper a CoMFA study of 28 MDR reversing compounds from the propafenone and benzofuran classes is reported. The results show a highly predictive power of the models when based on hydrophobic fields alone and in combination with steric and electrostatic fields. As previously suggested [9], in addition to the steric and electrostatic fields, the space directed hydrophobicity appears to be an important structural characteristic for explaining the differences in anti-MDR activity of the modulators from different chemical classes.

2 Materials and Methods

2.1 MDR reversing Activity

Data on MDR reversing activity *in vitro* in the T-lymphoblast cell line resistant to vincristine, CCRF-CEM/VCR-1000, were collected from papers of Ecker and coworkers [10,11]. This line is considered to display the "classic", i.e. P-gp associated MDR phenotype with a distinct expression of P-gp, no mutation at codon 185 and no significant contribution of other mechanisms to the cell resistance [10,12]. Two different criteria for estimating anti-MDR activity were applied: MTT assay of daunomycin cytotoxicity and inhibition of rhodamine-123 (Rh) efflux activity in presence of the modifiers. Although found to be highly intercorrelated ($R^2 = 0.895$ [10]) each of them was studied separately as giving a different assessment of the activity investigated. Both criteria were expressed as IC_{50} and logarithmic values of the inverse IC_{50} were used in the analyses. The reported activity values for the overlapping compounds (9 in all) on the same tumor cell line and the same MDR reversing assessments differ in the two studies. Therefore, principal component analysis (PCA) was used to combine both data sets, so that no priority to be given to one of them. Based on the correlation of $\log(1/EC_{50})$ values extracted by the first principal component the activity data from [11] were aligned to those of [10]. Table 1 shows the IC_{50} values of the compounds studied as taken from [10,11] and calculated by PCA. The values vary from -1.075 to 1.301 log units for the MTT assay and from -1.843 to 1.222 log units for the Rh-efflux.

2.2 Compounds

Two groups of propafenone-type MDR modulators were investigated. The first group consisted of 13 propafenone and 6 benzofuran derivatives collected from [10]. This group was basically used as a training set with its original activity data. The second group of 9 propafenone analogs was collected from [11] and was used as a test set with activity data calculated by PCA. In the final analyses both groups were used together with the PCA calculated activities for derivation of combined CoMFA models.

Table 1 lists the structures of the compounds investigated. In the table the same codes of the compounds are used as in the source papers [10,11] and the test compounds are preceded by "t_".

2.3 Computational Approaches

The PCA module of STATISTICA for Windows, V.5.1 was used for calculating the combined activity data. The molecular modeling calculations were done on a Silicon graphics workstation with SYBYL 6.3 molecular modeling software [13] using molecular mechanics (Tripos force field) and quantum chemistry (MOPAC V6: AM1). CoMFA calculations were performed with the Advanced CoMFA module of SYBYL and MOPAC was used as implemented in SYBYL. The HINT (Hydropatic INTeraction) program [14,15] was used for the calculation of the hydrophobic fields.

2.4 Starting Geometries and Geometry Optimization of 3D Structures of the Compounds

As no x-ray structural information was available for the investigated compounds a substructural search was performed in the Cambridge structural database V. 2.3.7 [16] in order to find relevant substructures of the most active compounds **1l** and **2c** respectively in the propafenone and benzofuran classes of the training set (Table 1). The substructural search of **1l** was done for two substructures. The first one contained the phenylethyl moiety, carbonyl group, benzene ring and the ether oxygen attached to it and was found in the x-ray structure with refcode KAWXIP. The second substructure presented the o-methylphenyl-piperazine moiety and was found in the x-ray structure with refcode BZALPZ. The starting geometry

Table 1. Structural and MDR reversing activity data of the compounds used in the study.

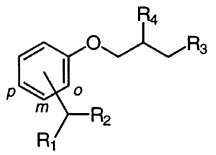

1

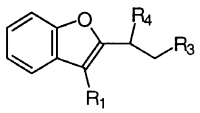

2

Compound	R_1[a]	R_2[a]	R_3	R_4	EC_{50} [μMol/l] Rhodamine-123 efflux Ref. 10	Rhodamine-123 efflux Ref. 11	Rhodamine-123 efflux PCA	MTT assay Ref. 10	MTT assay Ref. 11	MTT assay PCA
1a	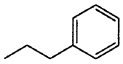	=O		−OH	3.55	2.30	3.55	0.29	0.46	0.29
1b	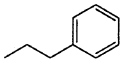	=O	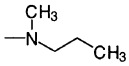	−OH	1.36	0.79	1.37	0.27	—	0.27
1c	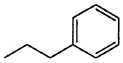	=O		−OH	7.12	5.01	7.11	0.82	3.67	0.90
1d	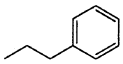	=O	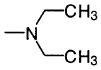	−OH	1.40	—	1.40	0.39	—	0.39
1e	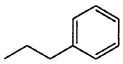	=O	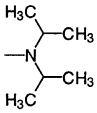	−OH	0.61	0.32	0.61	0.29	0.44	0.29
1f	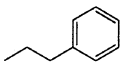	=O	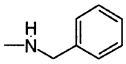	−OH	0.41	—	0.41	0.19	—	0.19
1g	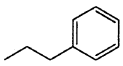	=O		−OH	2.55	1.59	2.55	0.52	—	0.52
1h	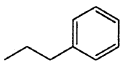	=O		−OH	1.65	0.98	1.66	0.29	0.28	0.25
1i	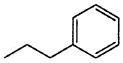	=O		−OH	13.56	10.30	13.53	1.49	6.19	1.43
1j	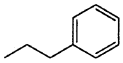	=O	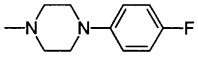	−OH	0.16	0.07	0.16	0.15	0.23	0.17
1k	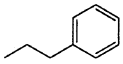	=O	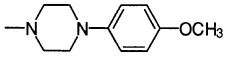	−OH	0.28	—	0.28	0.11	—	0.11
1l	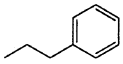	=O	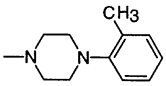	−OH	0.06	—	0.06	0.05	—	0.05
1m	$-CH_3$	=O	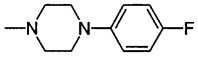	−OH	8.61	6.19	8.59	0.89	—	0.89
2a		−OH	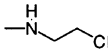	−OH	69.60	—	69.60	4.19	—	4.19

(*continued*)

Table 1. (*continued*)

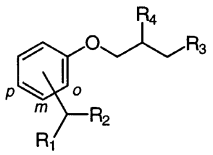

1

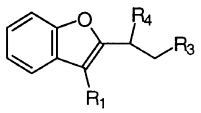

2

Compound	R_1[a]	R_2[a]	R_3	R_4	EC_{50} [μMol/l] Rhodamine-123 efflux Ref. 10	Rhodamine-123 efflux Ref. 11	Rhodamine-123 efflux PCA	MTT assay Ref. 10	MTT assay Ref. 11	MTT assay PCA
2b	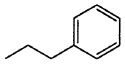	−OH	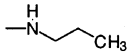	−OH	13.61	—	13.61	1.80	—	1.80
2c	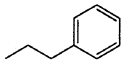	−OH	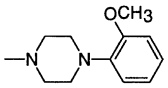	−OH	0.46	—	0.46	0.21	—	0.21
2d	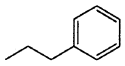	−H	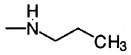	−H	2.90	—	2.90	0.87	—	0.87
2e	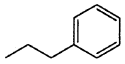	−H	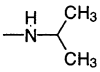	−H	5.80	—	5.80	1.10	—	1.10
2f	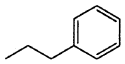	=O	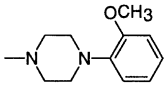	=O	4.96	—	4.96	2.02	—	2.02
t_11		=O		−OH	—	39.81	45.00	—	11.89	2.01
t_6a	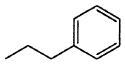	−OH		−OH	—	3.05	4.57	—	2.06	0.71
t_6b	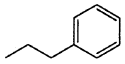	−OH	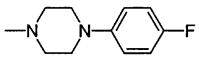	−OH	—	0.68	1.20	—	0.69	0.37
t_7a	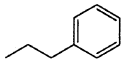	$-OCH_3$		−OH	—	0.99	1.68	—	0.55	0.32
t_7b	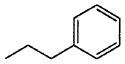	$-OCH_3$	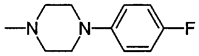	−OH	—	0.23	0.46	—	0.85	0.42
t_8a	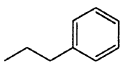 [b]	=O [b]		−OH	—	1.99	3.12	—	0.85	0.42
t_8b	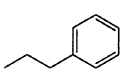 [b]	=O [b]	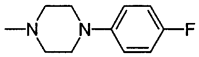	−OH	—	2.24	3.47	—	0.87	0.42
t_9a	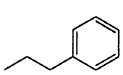 [c]	=O [c]		−OH	—	6.61	9.09	—	2.40	0.77
t_9b	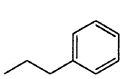 [c]	=O [c]	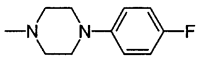	−OH	—	6.17	8.55	—	1.39	0.56

[a] all propafenone type compounds are *ortho*-substituted unless specially noted; [b] *meta*-substituted; [c] *para*-substituted

of **1l** was built by joining the respective x-ray substructures. A benzofuran ring x-ray structure was taken from the compound with refcode BZBARO. The starting structure of **2c** was built from the benzofuran ring and the remaining parts of the structures were joined to the ring as it was done for **1l**. Both starting conformations were then energy minimized using Tripos force field (Powell method, no electrostatics, and 0.05 kcal/mol*Å energy gradient convergence criteria).

The subsequent geometry optimization of the minimized structures of **1l** and **2c** were performed taking into account the following considerations: (i) the investigated compounds possess a high degree of conformational flexibility; (ii) as a close correlation between the membrane interacting and MDR reversing activity of the compounds studied was found [10] the lowest energy conformers, in which the benzyl and phenylethyl moieties are suitably extended, are preferable suggesting membrane-mediated interactions in the MDR reversal by these drugs [17]. Therefore, the systematic conformational search on the minimized structures of **1l** and **2c** was performed in two steps. In the first step the benzene/benzofuran ring with the N-substituted moiety in an extended conformation was kept as an aggregate and all rotatable bonds (four in **1l** and three in **2c**) in the remaining substructure were rotated with 30 degree increments (Figure 1, step 1). 12796 and 1001 conformations were obtained for **1l** and **2c**, respectively. From the conformational search local energy minima were extracted using an own version of the FAMILY program [18]. This resulted in 56 and 12 conformations for **1l** and **2c** respectively. These conformations were systematically compared and two of them were chosen for further analysis giving preference to suitably extended conformations with the highest shape similarity. In the second step the benzene/benzofuran ring and the phenylethyl moiety was kept as an aggregate and all rotatable bonds up to the basic nitrogen (five in **1l** and three in **2c**) were rotated with 30 degree increments (Figure 1, step 2). From the output of 62326 and 958 conformations the FAMILY program selected 40 and 12 local energy minima conformers for **1l** and **2c** respectively in an energy range of 10 kcal/mol above the global minimum found. As in the first step the remaining conformations were systematically compared and two of them were selected with suitably extended benzene/benzofuran and N-substituted moieties and the highest shape similarity. The structures of the other compounds were built based on the selected conformations of compounds **1l** and **2c**.

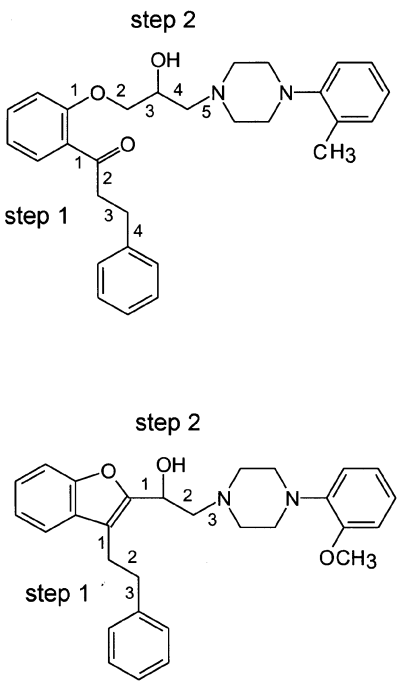

Figure 1. A stepwise systematic conformational search on **1l** and **2c** compounds with the rotatable bonds numbered.

All structures were minimized with molecular mechanics (Powell method, no electrostatics, and 0.05 kcal/mol*Å energy gradient convergence criteria) and charges were calculated using the MOPAC AM1 semiempirical quantum-chemical method.

2.5 Alignment of the Structures

Two different alignment rules were applied. The first one, called *Ar–O–N*, considers the substructure that is constantly presented in all molecules – the benzene ring, the oxygen atom (the ether oxygen in the propafenones and the furan oxygen in the benzofurans) and the basic nitrogen (Figure 2a). The second rule, called *Ar–Ar–N*, considers the role of the second aromatic ring present in the phenylethyl moiety and is done on the fitting of the centroids of the main benzene and phenylethyl moiety aromatic rings and the basic nitrogen (Figure 2b). The structures having no second aromatic ring (**1m, 2a, t_1l**) were aligned on the carbon atoms of the benzene ring and the basic nitrogen. In that case the aromatic carbon pairs were given weights of 1 and the nitrogen atom pair was given a weight of 6 to equally contribute to the alignment. In both alignments compound **1l** was the template molecule. In addition to the main alignment technique used (rms fit) the CoMFA field fit alignment based on the steric and electrostatic fields of **1l** was applied and the corresponding models calculated.

2.6 CoMFA Specifications

The following standard CoMFA characteristics were used: 2 Å regular grid spacing in all three dimensions within the defined region; 4 Å extension of the region beyond the van der Waals volumes of the best view oriented molecule; a sp^3

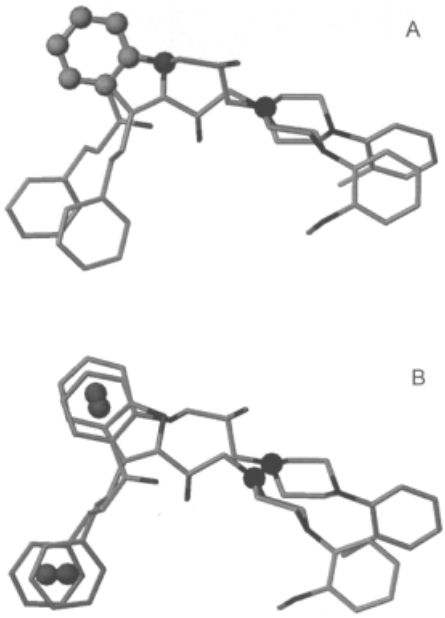

Figure 2. a: alignment *Ar–O–N* by the aromatic carbons, oxygen and nitrogen atoms (in balls); b: alignment *Ar–Ar–N* by the centroids of the aromatic rings and nitrogen atom (in balls); template molecule – **1l**; target molecule – **2c**; alignment technique – rms fit.

carbon probe atom with +1 charge; a distance dependent (1/r) dielectric constant. The following standard CoMFA fields were calculated: steric (S), electrostatic (E), and both (B). The indicator molecular and hydrogen-bond fields were also calculated. The same grid was used for all fields. In all calculations (if not especially stated) the standard energetic field cutoff value of 30 kcal/mol with no electrostatic interactions at bad steric contacts (drop electrostatics within steric cutoff for each row) and a threshold column filtering (σ_{min}) of 0.2 kcal/mol were used.

The CoMFA QSAR equations were calculated by PLS leave-one-out cross-validation procedure. The models were estimated by the cross-validated R squared, Q^2_{cv}, the optimal number of components, N_{opt}, and the standard error of prediction, SEP_{cv}. Additionally the contributions of the different fields were recorded. PLS uncross-validated runs were performed and used to predict the anti-MDR activity of the test compounds. The actual (PCA calculated) versus predicted activities of the test compounds were fitted by linear regression and the explained variance R^2, s and F ratio were recorded.

2.7 HINT Specifications

The HINT program [15] was used for the calculation of molecular lipophilic fields. Two kinds of hydrophobic fields were examined: hydrophobic/polar (H) and hydrophobic only (Ho). For H fields positive and negative values represent hydrophobic and hydrophilic regions respectively, while for Ho fields all negative values are truncated to zero. Both fields, H and Ho, were calculated without cutoff inside the molecules setting the polar proximity via bonds and treating all hydrogens. The same region was used for the hydrophobic fields as for the standard CoMFA fields.

3 Results and Discussion

The 3D-QSAR models derived from the training on 19 MDR modulators (compounds 1a-2f, Table 1) are presented in Table 2 and Table 3 for the *Ar–O–N* and *Ar–Ar–N* alignments respectively. Models were calculated for each field alone and in combination with the other fields to investigate the influence of a given molecular property and to find out those that yield the best predictive models. The maximum number of components was set to be either 10 or 15 in the first cross-validated PLS run and was subsequently decreased following the change in Q^2_{cv} and SEP_{cv}. During this decreasing several local optima of Q^2_{cv} for some of the models were found. The lowest N_{opt} were selected for the final cross-validated models (about 5 in most cases) providing the decrease in Q^2_{cv} was less than 0.05 from that obtained with the higher N_{opt}.

For both alignments the highest Q^2_{cv} were obtained with the hydrophobic fields (Ho and H) alone and in combination with steric (S) and steric plus electrostatic (both, B) fields, whereas the electrostatic (E) fields alone gave the models with the poorest predictivity (Tables 2 and 3). The neutral forms of the compounds were considered in the models as our experience from the CoMFA study on phenothiazines and related drugs showed that the models based on the neutral forms of the catamphiphilic drugs yielded higher Q^2_{cv} than those based on the protonated forms [9]. Additionally, the neutral forms of the compounds seem to be the more preferable forms considering membrane-mediated interactions in MDR reversal and the inside membrane location of the P-gp substrate binding sites [3,17,19].

As seen from the tables the *Ar–Ar–N* alignment (Table 3) improves Q^2_{cv} and reduces N_{opt} in comparison with the *Ar–O–N* one (Table 2) in most cases for both, MTT and Rh-efflux assays and the same models, namely Ho, S&Ho, and B&Ho, are the best for both criteria (presented in bold in Table 3). An increase in Q^2_{cv} (on average about 0.1) is observed for the standard CoMFA fields and their combinations with the hydrophobic fields. This observation can be considered as an indirect indication of the important role of the second aromatic ring when considered in relation to main aromatic ring and the basic nitrogen for the activities investigated. The necessity of the presence of more than one aromatic ring in the structures of the MDR-modulators was suggested by several authors and was related by them to the increase in lipophilicity. However,

Table 2. CoMFA models derived from the training of 19 *Ar–O–N* aligned compounds [10]; the first three models with the highest Q^2_{cv} are presented in bold.

MTT cytotoxicity assay							Rhodamine-123 efflux assay						
Model	Q^2_{cv}	N_{opt}	SEP_{cv}	Contribution, %			Model	Q^2_{cv}	N_{opt}	SEP_{cv}	Contribution, %		
				ster	ele	lipo					ster	ele	lipo
rms fit							rms fit						
S	0.654	3	0.315	100			S	0.530	4	0.579	100		
E	0.358	3	0.429		100		E	0.179	4	0.781		100	
B	0.704	4	0.302	51	49		B	0.548	4	0.579	53	47	
H	0.769	5	0.277			100	**H**	**0.646**	**13**	0.858			100
Ho	**0.848**	**4**	0.216			100	**Ho**	**0.800**	**10**	0.510			100
S & H	0.749	4	0.278	55		45	S & H	0.603	4	0.543	58		42
S & Ho	**0.789**	**5**	0.264	51		49	**S & Ho**	**0.660**	**4**	0.502	54		46
E & H	0.645	4	0.330		52	48	E & H	0.393	4	0.671		50	50
E & Ho	0.708	4	0.299		47	53	E & Ho	0.517	4	0.599		46	54
B & H	0.745	4	0.280	37	35	28	B & H	0.556	4	0.574	40	32	28
B & Ho	**0.781**	**4**	0.260	35	34	31	B & Ho	0.635	4	0.521	36	33	31
field fit							field fit						
S	0.734	3	0.276	100			S	0.610	5	0.559	100		
E	0.289	4	0.468		100		E	0.290	7	0.819		100	
B	0.749	4	0.278	54	46		**B**	**0.652**	**6**	0.549	52	48	
H	**0.820**	**7**	0.265			100	H	0.581	6	0.602			100
Ho	**0.795**	**4**	0.251			100	Ho	0.643	5	0.534			100
S & H	**0.797**	**6**	0.270	52		48	**S & H**	**0.676**	**9**	0.611	56		44
S & Ho	0.781	4	0.259	59		41	S & Ho	0.640	4	0.517	55		45
E & H	0.732	9	0.358		53	47	E & H	0.490	9	0.768		57	43
E & Ho	0.705	7	0.340		53	47	E & Ho	0.529	4	0.591		54	46
B & H	0.784	4	0.258	35	35	30	B & H	0.635	6	0.562	37	34	29
B & Ho	**0.797**	**4**	0.250	35	36	29	**B & Ho**	**0.660**	**4**	0.502	36	36	28

the models based on the standard CoMFA fields show an increase in Q^2_{cv} , while a slight decrease in Q^2_{cv} is observed for some H and Ho based models in the *Ar–Ar–N* alignment. As in CoMFA the molecules are suggested to be aligned according to a possible pharmacophoric pattern, the better results with the *Ar–Ar–N* alignment thus presume indirectly the potential involvement of the second aromatic ring in receptor specific interactions in addition to its influence on lipophilicity of the compounds studied.

Another interesting observation relates to differences in the quality of the models based on MTT assay and Rh-efflux data. CoMFA models with higher predictivity were obtained for the MTT assay than for the Rh-efflux assay (Tables 2 and 3). According to [10] the rhodamine-123 efflux is a more direct method for measuring interaction with P-gp, and the MTT assay represents a more general assay for the modulation of MDR, which accounts additionally for intracellular metabolism of the modulators. In parallel with the intracellular metabolism one can also suggest, that the MTT assay accounts for involvement of additional mechanisms of MDR reversal different from a direct binding to P-gp, particularly compound-membrane interactions. A high correlation was reported between differential scanning calorimetry data on interactions of the compounds within a homologous series of propafenones with membrane phospholipids and their biological activity [10]. Also our previous investigations pointed to the role of the drug-membrane interactions for the anti-MDR activity of catamphiphiles [17]. According to the model proposed for the functioning of P-gp as an efflux pump [2], the antitumor drugs and respectively their competitors, could bind to P-gp being still in the membrane, i.e. before entering the cell and reaching any intracellular target. It has also been shown by kinetic analysis [20] that the cytotoxic agents and P-gp substrates can bind to separate sites, and that the reverters can bind competitively to one site and uncompetitively to other sites. Thus, even suggesting the direct binding to P-gp to be the main mechanism of MDR reversal by these compounds, the MTT assay, as considering the increase in cytotoxicity, is the more relevant assessment of anti-MDR activity and correlates better with the space molecular properties of the compounds studied. However, it should be stated that both criteria gave models with high predictive power and the models with the same fields are the best for both, MTT cytotoxicity and Rh efflux.

A more detailed comparison of the models in Table 2 and 3 reveals that the MTT assay data show better Q^2_{cv} for the field fit aligned molecules and Rh-efflux data for the rms fit

Table 3. CoMFA models derived from the training of 19 *Ar–Ar–N* aligned compounds [10]; the first three models with the highest Q^2_{cv} are presented in bold.

MTT cytotoxicity assay							Rhodamine-123 efflux assay						
Model	Q^2_{cv}	N_{opt}	SEP_{cv}	Contribution, %			Model	Q^2_{cv}	N_{opt}	SEP_{cv}	Contribution, %		
				ster	ele	lipo					ster	ele	lipo
rms fit							rms fit						
S	0.709	3	0.289	100			S	0.670	3	0.478	100		
E	0.363	3	0.428		100		E	0.347	3	0.673		100	
B	0.711	3	0.288	61	39		B	0.654	3	0.489	63	37	
H	0.758	5	0.283			100	H	0.637	5	0.539			100
Ho	**0.848**	**3**	0.209			100	**Ho**	**0.779**	**3**	0.392			100
S & H	0.795	6	0.271	58		42	S & H	0.682	3	0.469	57		43
S & Ho	**0.839**	**6**	0.241	56		44	**S & Ho**	**0.743**	**3**	0.422	56		44
E & H	0.654	3	0.315		50	50	E & H	0.586	3	0.535		56	44
E & Ho	0.714	3	0.287		58	42	E & Ho	0.681	3	0.470		52	48
B & H	0.770	3	0.257	43	26	31	B & H	0.672	3	0.477	44	25	31
B & Ho	**0.812**	**5**	0.249	42	27	31	**B & Ho**	**0.721**	**3**	0.439	42	24	34
field fit							field fit						
S	0.782	3	0.250	100			S	0.640	3	0.500	100		
E	0.419	3	0.408		100		E	0.218	3	0.736		100	
B	0.770	4	0.266	61	39		B	0.644	4	0.514	61	39	
H	0.771	5	0.276			100	H	0.588	5	0.574			100
Ho	**0.887**	**3**	0.180			100	**Ho**	**0.738**	**3**	0.426			100
S & H	0.774	4	0.263	60		40	S & H	0.618	3	0.515	60		40
S & Ho	**0.853**	**3**	0.205	57		43	**S & Ho**	**0.721**	**4**	0.432	56		44
E & H	0.746	9	0.349		54	46	E & H	0.508	3	0.584		51	49
E & Ho	0.797	4	0.250		51	49	E & Ho	0.655	3	0.489		58	42
B & H	0.802	9	0.307	42	27	31	B & H	0.620	4	0.531	42	28	30
B & Ho	**0.846**	**4**	0.218	42	28	30	**B & Ho**	**0.710**	**3**	0.448	41	27	32

aligned molecules. In fact, the field fit improves models that use the standard CoMFA fields as it does a fit of steric and electrostatic fields by minimizing the differences at each lattice point between the template molecule and the other molecules in the set. It is considered in the literature that alignment based on the field fit for predicting binding constants is an artifact rather than a real result as it minimizes the entropic contributions of the free energy of binding by putting the aligned molecules to share a common global shape and location in the 3D lattice [21]. Thus, one can speculate that the better results obtained by the rms fit for Rh-efflux data are reasonable taking into account that this assessment is more directly related to the ability of the reverters to bind to P-gp as the MTT assay.

An excellent correlation between the lipophilicity expressed as log P calculated by the program MOLGEN and Rh-efflux inhibition activity was reported for the homologues series of propafenone and benzofuran analogs [10]. However, log P failed to predict the anti-MDR activity of both classes taken together. Correlating the calculated log P values of all 19 compounds with any of the MDR reversing criteria used, extremely low cross-validated R^2 were obtained for MTT assay (0.02) and relatively low for Rh-efflux (0.31). Similar results were obtained using the log P values calculated by the program HINT: 0.09 and 0.41 for MTT and Rh-efflux assay respectively. Even without considering the compound 2f as done in [10] the cross-validated R^2 remains low (0.2 using MOLGEN values taken from [10]). The obtained CoMFA models, however, show that the hydrophobic fields alone and in combination with steric and electrostatic fields are able to explain the differences in anti-MDR activity of the modulators of different chemical classes (models Ho, S&Ho, B&Ho in Tables 2 and 3). Thus, similarly to the 3D-QSAR models of phenothiazines and related drugs [9], the models of propafenone-type MDR modulators of different classes show that hydrophobicity is a relevant property only if considered as a space directed molecular field.

To get some more insight about the specific properties related to anti-MDR activity two additional CoMFA fields were also investigated – indicator and H-bond fields.

Atom-based indicator variables were proposed in CoMFA as a tool for obtaining models of higher consistency. It was suggested that rather random energy values could be assigned to some lattice points in the vicinity of the compounds if one compares two identical molecules which are not perfectly superimposed. Subsequently the results of PLS analysis become significantly influenced by this

random alignment [22]. Therefore, we performed CoMFA with indicator steric type fields varying the energy cutoff values and grid spacing. The results obtained are presented in Table 4 for *Ar–Ar–N* aligned molecules. As seen from the table no improvement in Q^2_{cv} was observed compared to the standard CoMFA steric field. Setting lower grid spacings the number of columns used and the computational time, respectively, increased significantly without any win in the predictive Q^2_{cv}. The values were even lower in comparison to the standard steric field, remaining, however, higher than 0.6 and confirming in this way the consistency of the models obtained.

To investigate the possible H-bond acceptor/donor capabilities of the compounds studied the H-bond fields were also introduced. At present, donor and acceptor fields can not be separated computationally in SYBYL-CoMFA, however nominal (equal to the steric cutoffs) energies are assigned to the lattice points if they are close to H-bond accepting or donating atoms. Extremely low and even negative Q^2_{cv} values were observed varying the energy cutoffs in a large interval (Table 4). These results are in agreement with the low Q^2_{cv} obtained with the electrostatic fields and the poor correlation obtained by Ecker at al. with H-bond acceptor characteristics for N-4 of the piperazine ring in the N-substituted moiety reported recently for compounds of the same propafenone class [23].

To test the obtained models 9 compounds of the propafenone class taken from [11] were used. The reported activity data for the overlapping compounds differed in [10] and [11] (Table 1). Therefore, the activity values of the test compounds were calculated by PCA and considered to be their "observed" values in the test. The results of testing are summarized in Table 5. Figure 3 shows the plot of the predicted versus observed MTT assay values for the training set compounds obtained by the cross-validated field fit B&Ho model (Table 3). The close values of Q^2_{cv} and R^2 of the fitted line (0.846 and 0.855 respectively) point to the stability of the model obtained. The plot of the predicted versus observed (PCA calculated) MTT assay values for the test set compounds by the same uncross-validated B&Ho model with 4 components (Table 5) is presented in Figure 4. As seen from Table 5 and Figure 4 the prediction yields R^2 from 0.703 to 0.830 for the MTT assay in the field fit and from 0.703 to 0.766 for the Rh-efflux in the rms fit. All predictions are statistically significant and most of them have slopes of about 1.00. The intercepts of the fitted lines are higher than 0, pointing to some overprediction of the test compounds' activity.

To proof further the predictivity and consistency of the obtained 3D-QSAR models, the training was done combining both, training and test sets using the PCA calculated activity data. The results are presented in Table 6. The Q^2_{cv} values are comparable to those of the training on the 19 compounds from [10] and even a slight increase for some fields is observed. The best models combined the CoMFA standard and hydrophobic fields and again, the MTT assay based models had higher Q^2_{cv} than those based on the Rh-efflux data. These results demonstrate the good predictivity and stability of the derived CoMFA models.

Fig. 5 represents the CoMFA STDEV*COEFF contour plots obtained from the uncross-validated model B&Ho (Table 6) of the combined data set for the MTT assay data with the superimposed structures displayed. On the graphics the colored regions correspond to the differences in the compounds' fields that are most highly associated with the differences in anti-MDR activity. One should notice that, in general, the correct and content interpretation of the STDEV*COEFF contour plots is rather difficult as the CoMFA models obtained are always related to a given group of compounds with given activity. Thus, interpreting the graphical results, one should consider that they may reflect both, the structural variation of the data set, and/or

Table 4. CoMFA models of 19 *Ar–Ar–N* field fit aligned compounds [10] using steric indicator and H-bond fields.

	Energy cutoff	Grid spacing	Q^2_{cv}/N_{opt}		Grid points used
Field			MTT cytotoxicity assay	Rh-efflux inhibition	
Indicator	30	2	0.684/5	0.484/3	152
	30	1	0.724/3	0.609/3	1240
	30	0.75	0.718/3	0.605/3	2912
	20	2	0.671/4	0.599/9	157
	20	1	0.716/3	0.631/3	1286
	20	0.75	0.726/3	0.618/3	3019
H-bond	100	2	0.087/1	−0.163/1	74
	60	2	0.072/1	−0.178/1	68
	50	2	0.110/1	−0.129/1	67
	30	2	0.102/1	−0.117/1	65
	1	2	0.016/1	−0.125/1	25

Table 5. Results on prediction of the test set compounds [11] by the CoMFA models with the highest Q^2_{cv} as presented in Table 3.

				Training (no crossvalidation)			Test			
Activity	Model	Fit	N_{opt}	R^2	s	F	R^2	s	F	Intercept/Slope
MTT assay	Ho	rms	3	0.948	0.122	90.8	0.773	0.172	23.8	0.237/1.216
	S & Ho		6	0.996	0.037	520.6	0.736	0.183	19.5	0.205/1.169
	B & Ho		13[a]	1.000	0.000	$> 10^5$	0.740	0.152	19.9	0.167/0.983
	B & Ho		5	0.996	0.037	618.3	0.777	0.151	24.4	0.157/1.076
	Ho	field	3	0.970	0.092	164.1	0.703	0.205	16.6	0.355/1.024
	S & Ho		3	0.978	0.079	225.0	0.762	0.166	22.5	0.279/1.134
	B & Ho		8[a]	1.000	0.009	6021	0.789	0.127	26.2	0.246/0.940
	B & Ho		4	0.992	0.050	433.8	0.830	0.119	34.2	0.225/1.002
Rh-123 efflux assay	Ho	rms	3	0.926	0.227	62.1	0.703	0.381	16.5	0.69 /0.950
	S & Ho		3	0.985	0.103	319.4	0.766	0.353	23.0	0.621/1.039
	B & Ho		3	0.990	0.083	502.9	0.664	0.397	13.8	0.487/0.904
	Ho	field	3	0.963	0.161	128.9	0.534	0.445	8.0	0.738/0.730
	S & Ho		4	0.984	0.108	221.1	0.629	0.402	11.9	0.666/0.850
	B & Ho		3	0.941	0.202	79.5	0.618	0.370	11.3	0.321/0.762

[a]uncross-validation run and prediction results obtained with the highest number of optimal components found in the cross-validated run.

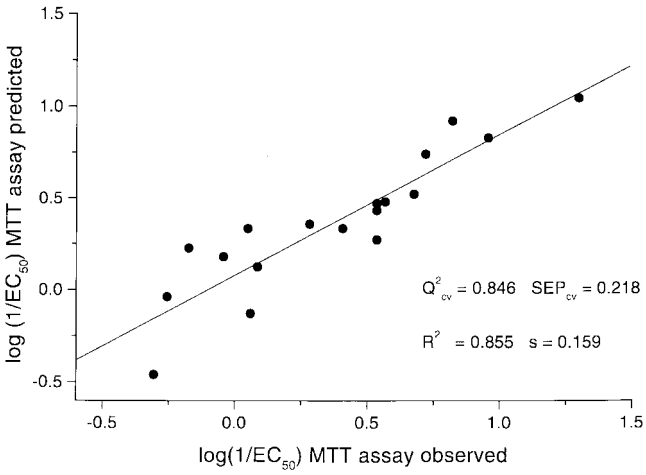

Figure 3. MTT assay values of the training set compounds predicted by the cross-validated field fit model B&Ho (Table 3) versus observed MTT assay values.

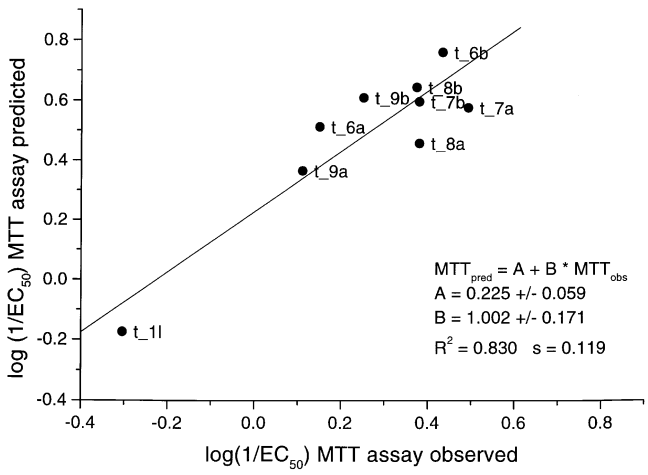

Figure 4. MTT assay values of the test set compounds predicted by the uncross-validated field fit model B&Ho with 4 components (Table 5) versus MTT assay values calculated by PCA (Table 1).

Table 6. CoMFA models derived from the combined data set of 28 *Ar–Ar–N* field fit aligned compounds [10, 11]; the first three models with the highest Q^2_{cv} are presented in bold.

MTT cytotoxicity assay							Rhodamine-123 efflux assay					
Model	Q^2_{cv}	N_{opt}	SEP_{cv}	Contribution, %			Model	Q^2_{cv}	N_{opt}	SEP_{cv}	Contribution, %	
				ster	ele	lipo					ster	ele	lipo
S	0.706	3	0.243	100	—	—	S	0.610	3	0.469	100	—	—
E	0.358	4	0.367	—	100	—	E	0.263	2	0.631	—	100	—
B	**0.804**	**6**	0.212	52	48	—	**B**	**0.680**	**4**	0.434	52	48	—
H	0.746	6	0.242	—	—	100	H	0.595	5	0.499	—	—	100
Ho	0.774	6	0.228	—	—	100	Ho	0.620	6	0.494	—	—	100
S & H	0.773	6	0.228	51	—	49	S & H	0.641	5	0.469	54	—	46
S & Ho	0.785	6	0.222	59	—	41	S & Ho	0.651	3	0.443	59	—	41
E & H	0.745	12	0.286	—	56	44	E & H	0.492	5	0.559	—	54	46
E & Ho	0.763	10	0.259	—	54	46	E & Ho	0.556	3	0.500	—	58	42
B & H	**0.816**	**6**	0.205	36	34	30	**B & H**	**0.674**	**5**	0.448	36	35	29
B & Ho	**0.835**	**6**	0.194	36	36	28	**B & Ho**	**0.706**	**3**	0.407	38	38	24

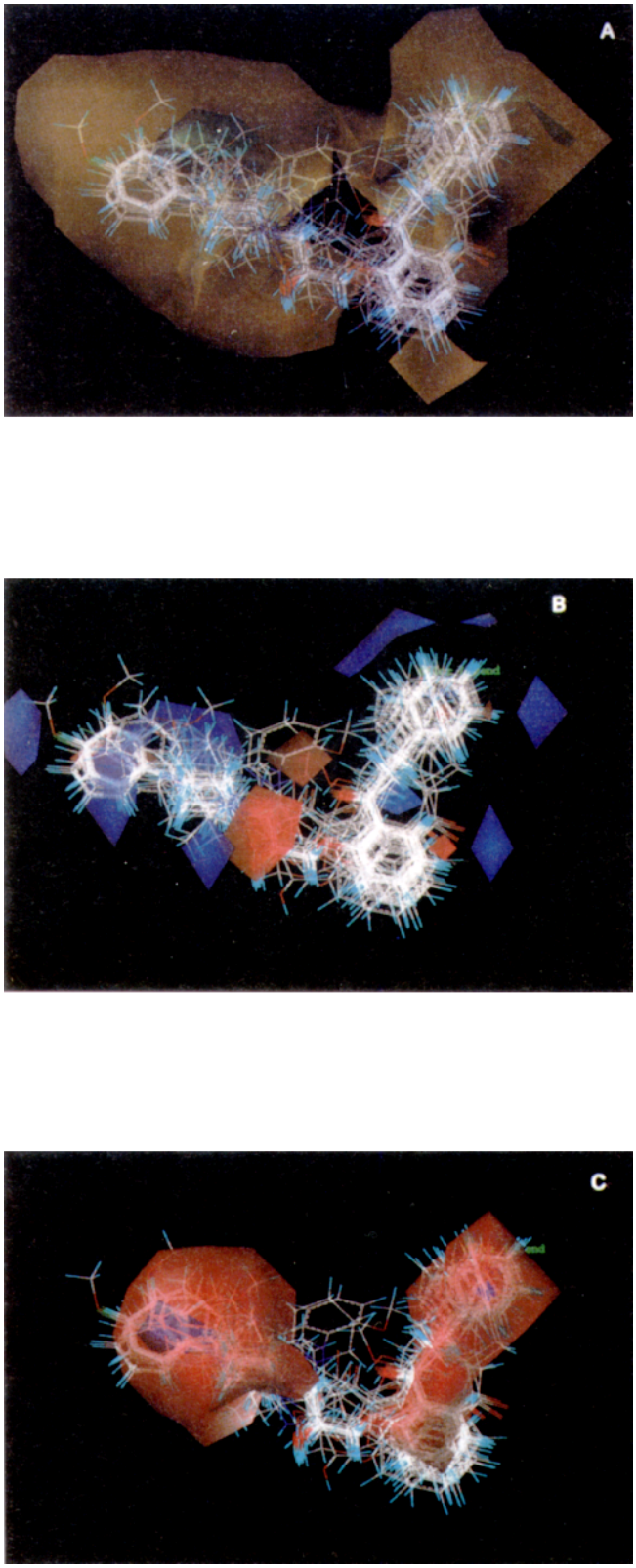

Figure 5. Graphical results as derived from the model B&Ho of the combined data set (MTT assay, Table 6) with the superimposed molecules displayed: A: steric fields; B: electrostatic fields; C: hydrophobic only fields.

the regions of possible importance for the activity investigated.

Large sterically forbidden regions (Figure 5a, in yellow) are displayed along the moieties in both directions of the benzene/benzofuran rings reflecting the sterical variation in the data set rather than important sterical regions. The same large sterically unfavaroble regions were observed as well in the models with S and steric B fields alone (data not shown), indicating, on one hand, that the hydrophobic and standard CoMFA fields are not intercorrelated and confirming, on the other hand, the consistency of the models obtained. The sterically favorable region (in green) apart from the basic nitrogen in the N-substituted moiety points to more bulky substituents in this place as necessary to obtain a higher MDR reversal effect. This observation is in agreement with our QSAR and CoMFA results on phenothiazines, thioxanthenes and related drugs on the favorable influence of more bulky substituents in the aliphatic chain, namely the piperazine-type N-substituted moiety [7,8,9]. The result can possibly be related to some given size and form (o-substituted aromatic ring attached to the piperazine ring) that the molecules must have at that place in order to fit better to the putative MDR reversal receptor or receptors. In contrast to the steric fields, the electrostatic ones are presented by small regions of low (in blue) and high (in red) electron density that are displayed mostly in the N-substituted part of the structures (Figure 5B). More negative charges around the R2 substituent (according to the designation in Table 1) is expected to increase anti-MDR activity, whereas less electron density is favorable around the R1 and R3 substituents. For the hydrophobic only (Ho) field (Figure 5C) the red regions represent areas where more hydrophobicity promotes favorable interactions and the blue ones discourages them. According to the graphics more lipophilic end parts of both moieties lead to higher activity values. In all graphics the important areas displayed are related mainly to both moieties whereas no contributing signal could be identified around the main "core" (benzene/benzofuran rings) of the structures. This observation corresponds to the alignment used and points as well to possible structural modifications in the moieties to get more active propafenone-type MDR modulators.

On the basis of the obtained 3D-QSAR models of propafenone-type MDR modulators several main conclusions could be drawn. The first one relates to the possibility of explaining the differences in anti-MDR activity of compounds of different classes if space directed molecular properties of the structures are considered. As for phenothiazines and related drugs [9] hydrophobicity appears to be a structural characteristic of importance for anti-MDR activity of the compounds studied. Although the MTT cytotoxicity and rhodamine123-efflux assays were

shown to be highly intercorrelated [10], their CoMFA give different predictive abilities. The MTT cytotoxicity assay, being the more relevant MDR reversal assessment, also yields better results when related to the molecular fields of the modulators studied.

References

[1] Ford, J. Modulators of multidrug resistance. *Hematology/Oncology Clinics of North America 9 (2)*, 337–361 (1995).

[2] Gottesman, M. M. How cancer cells evade chemotherapy: sixteenth Richard and Hinda Rosenthal Foundation award lecture. *Cancer Res. 53*, 747–754 (1993).

[3] Gottesman, M. M. and Pastan, I. Biochemistry of the multidrug resistance mediated by the multidrug transporter. *Ann. Rev. Biochem. 62*, 385–427 (1993).

[4] Ford, J. M., Prozialeck, W. C. and Hait, W. N. Structural features determining activity of phenothiazine and related drugs for inhibition of cell growth reversal of multidrug resistance. *Mol. Pharmacol. 35*, 105–115 (1989).

[5] Ramu, A and Ramu, N. Reversal of multidrug resistance by phenothiazines and structurally related compounds. *Cancer Chemother. Pharmacol. 30*, 165–173 (1992).

[6] Pearce, H. L., Winter, M. A. and Beck, W. T. Structural characteristics of compounds that modulate P-glycoprotein-associated multidrug resistance. *Adv. Enzyme Regulations 30*, 357–373 (1990).

[7] Pajeva, I. K. and Wiese, M. QSAR and molecular modeling of catamaphilic drugs able to modulate multidrug resistance in tumors. *Quant. Struct.-Act. Relat. 16*, 1–10 (1997).

[8] Wiese, M. and Pajeva, I. K. Molecular modeling study of the multidrug resistance modifiers cis- and trans-flupentixol. *Pharmazie 52*, 679–685 (1997).

[9] Pajeva, I. K. and Wiese, M. Molecular modeling of phenothiazines and related drugs as multidrug resistance modifiers: a comparative molecular field analysis study. *J. Med. Chem. 41*, 1815–1826 (1998).

[10] Ecker, G., Chiba, P., Hitzler, M., Schmid D., Visser, K., Cordes H.-P., Csöllei J., Seydel J. K. and Schaper, K.-J. Structure-Activity Relationship Studies on Benzofuran Analogs of Propafenone-Type Modulators of Tumor Cell Multidrug Resistance. *J. Med. Chem. 39*, 4767–4774 (1996).

[11] Chiba, P., Ecker, G., Schmid, D., Drach, B., Tell, B., Goldenberg, S., and Gekeler, V. Structural Requirements for Acitvity of Propafenone-type Modulators in P-Glycoprotein-Mediated Multidrug Resistance. *Mol. Pharmacol. 49*, 1122–1130 (1996).

[12] Zamora, J. M., Pearce, H. L. Beck, W. T. Physical-Chemical Properties Shared by Compounds that Modulate Multidrug resistance in Human Leukemic Cells. *Mol. Pharmacol. 33*, 454–462 (1988).

[13] Tripos Ass., 1699 Hanley Road, St. Louis, Mo 63144, USA.

[14] Kellog, G. E., Semus, S. F. and Abraham, D. J. HINT: A new method for empirical hydrophobic field calculation for CoMFA. *J. Comp.-Aided Mol. Design 5*, 545–552 (1991).

[15] Edusoft, LC, PO Box 1811, Ashland, VA 23005, USA.

[16] Cambridge Crystallographic Data Centre, V. 5.13, University Chemical Laboratory, Lensfield Road, Cambridge CB2 1EW, U.K.

[17] Pajeva, I. K., Wiese, M., Cordes, H.-P. and Seydel, J. K. Membrane interactions of some catamphiphilic drugs and relation to their multidrug-resistance-reversing ability. *J. Cancer Res. Clin. Onc. 122*, 27–40 (1996).

[18] Mauerhofer, E. and Höltje, H.-D. *First Workshop on Molecular Modelling*, May 1987, Darmstadt.

[19] Garnier-Suillerot, A. Impaired accumulation of drug in multidrug resistant cells. What are the respective contributions of the kinetics of uptake of P-glycoprotein-mediated efflux of drug? *Curr. Pharmaceut. Design 1*, 69–82 (1995).

[20] Safa, A. Identification and characterization of the drug-binding sites of P-glycoprotein, in: Gupta, S. and Tsuruo, T. (Eds), *Multidrug Resistance in Cancer Cells*, J. Wiley & Sons, Chichester 1996, pp. 231–249.

[21] Folkers, G., Merz, A. and Rognan, D. CoMFA: Scope and limitations, in: Kubinyi, H. (Ed.) *3D QSAR in Drug Design. Theory, Methods and Application*, Escom, Leiden 1993, pp. 583–618.

[22] Kroemer, R. T. and Hecht, P. Replacement of steric 6-12 potential-derived interaction energies by atom-based indicator variables in CoMFA leads to models of higher consistency. *J. Comp.-Aided Mol. Design 9*, 205–212 (1995).

[23] Chiba, P., Hitzler, M., Richter, E., Huber, M., Tmej, C., Giovagnoni, E. and Ecker, G. Studies of propafenone-type modulators of multidrug resistance III: variations on the nitrogen *Quant. Struct.-Act. Relat. 16*, 361–366 (1997).

Received on January 27, 1998; accepted on March 24, 1998